Trans-α-glucosylation of stevioside by the mutant glucansucrase enzyme Gtf180-ΔN-Q1140E improves its taste profile

Tim Devlamynck[a,b], Evelien M. te Poele[a,1], Koen Quataert[b], Gerrit J. Gerwig[a,c], Davy Van de Walle[d], Koen Dewettinck[d], Johannis P. Kamerling[a,c], Wim Soetaert[b], Lubbert Dijkhuizen[a,1,*]

[a] Microbial Physiology, Groningen Biomolecular Sciences and Biotechnology Institute (GBB), University of Groningen, Nijenborgh 7, 9747 AG Groningen, The Netherlands
[b] Centre for Industrial Biotechnology and Biocatalysis, Department of Biochemical and Microbial Technology, Faculty of Bioscience Engineering, Ghent University, Coupure Links 653, 9000 Ghent, Belgium
[c] NMR Spectroscopy, Bijvoet Center for Biomolecular Research, Utrecht University, Padualaan 8, 3584 CH Utrecht, The Netherlands
[d] Laboratory of Food Technology and Engineering, Faculty of Bioscience Engineering, Ghent University, Coupure Links 653, 9000 Ghent, Belgium

ARTICLE INFO

ABSTRACT

The adverse health effects of sucrose overconsumption, typical for diets in developed countries, necessitate use of low-calorie sweeteners. Following approval by the European Commission (2011), steviol glycosides are increasingly used as high-intensity sweeteners in food. Stevioside is the most prevalent steviol glycoside in *Stevia rebaudiana* plant leaves, but it has found limited applications in food products due to its lingering bitterness. Enzymatic glucosylation is a strategy to reduce stevioside bitterness, but reported glucosylation reactions suffer from low productivities. Here we present the optimized and efficient α-glucosylation of stevioside using the mutant glucansucrase Gtf180-ΔN-Q1140E and sucrose as donor substrate. Structures of novel products were elucidated by NMR spectroscopy, mass spectrometry and methylation analysis; stevioside was mainly glucosylated at the steviol C-19 glucosyl moiety. Sensory analysis of the α-glucosylated stevioside products by a trained panel revealed a significant reduction in bitterness compared to stevioside, resulting in significant improvement of edulcorant/organoleptic properties.

1. Introduction

Over the past decade, Western society has increasingly been confronted with lifestyle diseases, such as type 2 diabetes, ischaemic heart attacks and various cardiovascular problems. The cost for society in Europe is estimated to be 2 to 4% of the total healthcare cost (WHO, 2007). The risk of suffering from lifestyle diseases increases significantly when the BMI is higher than $25 \, \text{kg/m}^2$ (Field et al., 2001; Gregg et al., 2005). A study by Calle, Rodriguez, Walker-Thurmond, and Thun (2003) revealed that 14 to 20% of all cancer deaths may be related to overweight or obesity. Important causes of overweight are a decrease of physical activity and inappropriate dietary patterns. Moreover, an excessive sugar intake appears to be directly associated with an increase in body weight (Te Morenga, Mann, & Mallard, 2013). Consequently, a wider array of sweet food products with less or even no sugar content is a necessity in order to reduce the prevalence of lifestyle diseases.

Consumers are more and more aware of the relationship between diet-related diseases and healthy foods but are nevertheless not eager to decrease their intake of sweet food products (Sun, 2008). In addition, the 'natural' character of the applied sweeteners is increasingly perceived by consumers to be equally important as their taste (Bearth, Cousin, & Siegrist, 2014). The implementation of natural, high-intensity sweeteners is thus driven by a strong consumer demand. To date, several candidates have been proposed to assume this role: sweet-tasting proteins, such as monatin and thaumatin (Faus, 2000), and plant extracts, such as glycyrrhizin from the root of *Glycyrrhiza glabra* (Liu, Sugimoto, Akiyama, & Maitani, 2000), mogrosides from monk fruit (*Siraitia grosvenorii*) (Murata et al., 2006), and steviol glycosides from the leaves of the *Stevia rebaudiana* plant (Goyal, Samsher, & Goyal, 2010). Since the European Commission (EU Commission, 2011) authorized the use of high purity steviol glycosides ($\geq 95\%$), such as rebaudioside A (RebA) and stevioside (Stev), in foods and beverages, stevia-based products have rapidly expanded across the European

market. By means of their steviol group, steviol glycosides potentiate Ca^{2+}-dependent activity of TRPM5, a cation channel protein essential for taste transduction of sweet, bitter and umami in chemosensory cells (Prawitt et al., 2003). As a result, the perception of the sweetness of steviol glycosides is intensified, along with a lingering bitterness. Interestingly, TRPM5 also facilitates insulin release by the pancreas, preventing high blood glucose concentrations and consequently the development of type 2 diabetes (Colsoul et al., 2010). A study on mice revealed that TRPM5 potentiation by steviol glycosides protected them against the development of high-fat diet-induced hyperglycaemia, prompting the authors to propose steviol glycosides as cost-effective antidiabetic drugs (Philippaert et al., 2017).

Unfortunately, the lingering bitterness of RebA and Stev is experienced by roughly half of the human population, as reflected by considerable sequence variation in the genes encoding for the bitter receptors hTAS2R4 and hTAS2R14 (Hellfritsch, Brockhoff, Stähler, Meyerhof, & Hofmann, 2012). One strategy to solve this issue consists in the addition of masking agents such as several sugar alcohols (Sips & Vercauteren, 2011). In order to circumvent the use of masking agents, enzymatic glycosylation of RebA and Stev has been proposed as a means to (partially) remove their bitterness (see review by Gerwig, te Poele, Dijkhuizen, & Kamerling, 2016). Several enzymes, typically UDP-glucosyltransferases (UGTases) (Wang et al., 2015) and cyclodextrin glucanotransferases (CGTases) (Abelyan, Balayan, Ghochikyan, & Markosyan, 2004; Yu, Yang, Li, & Yuan, 2015), have been applied for this purpose. However, UGTases require expensive nucleotide-activated sugars as donor substrates (Desmet et al., 2012), whereas CGTases possess poor C-13/C-19 regiospecificity, producing mixtures of α-glucosylated steviol glycosides (Abelyan et al., 2004).

Alternatively, glucansucrases can be applied for the α-glucosylation of steviol glycosides. Glucansucrases (EC 2.1.4.-) are enzymes found only in lactic acid bacteria, of which most members, including *Lactobacillus reuteri*, have the generally-recognized-as-safe (GRAS) status. They use the donor substrate sucrose to catalyze the synthesis of α-glucan polysaccharides, thereby introducing different ratios of glycosidic linkages, depending on the enzyme specificity (Leemhuis et al., 2013). In previous studies, we have demonstrated that suppressing this α-glucan synthesis by mutational engineering of the Gtf180-ΔN glucansucrase of *Lactobacillus reuteri* strain 180 improved trans-α-glucosylation of non-natural acceptor substrates such as catechol (Devlamynck, te Poele, Meng, van Leeuwen, & Dijkhuizen, 2016). Recently, we reported the trans-α-glucosylation of RebA with the Q1140E mutant of the Gtf180-ΔN glucansucrase (te Poele et al., 2018). This steviol glycoside was only α-glucosylated at the steviol C-19 glucosyl moiety, producing mainly a mono-glucosylated product with an (α1 → 6) linkage, but also products with two or more α-glucosyl units attached. The glucosylation of Stev, the most abundant steviol glycoside in *Stevia rebaudiana* leaves, was not addressed. Here, we report a careful optimization of the enzymatic glucosylation of Stev by the same glucansucrase mutant enzyme. The structures of the main α-glucosylated Stev products were characterized by NMR spectroscopy, mass spectrometry and methylation analysis. Sensory analysis by a trained panel revealed a substantial decrease in bitterness and off-flavours of the α-glucosylated products compared to Stev and RebA.

2. Materials and methods

2.1. Commercial steviol glycosides

Stevioside (Stev, > 85% purity, HPLC) was obtained from TCI Europe, Belgium, and steviolbioside (SB) from Wako Chemicals GmbH, Germany.

2.2. Production and purification of recombinant Gtf180-ΔN-Q1140E enzyme

Recombinant, N-terminally truncated glucansucrase Gtf180-ΔN from *Lactobacillus reuteri* 180 and the derived Q1140E mutant were produced and purified as described previously (Kralj et al., 2004; te Poele et al., 2018).

2.3. Gtf180-ΔN-Q1140E enzyme activity assays

Enzyme activity assays were performed at 37 °C with 100 mM sucrose in 25 mM sodium acetate (pH 4.7), containing 1 mM $CaCl_2$. Samples of 150 μl were taken every min over a period of 8 min, and immediately inactivated with 30 μl of 1 M NaOH. The sucrose, glucose and fructose concentrations of the samples were subsequently quantified by means of HPLC analysis, allowing the calculation of the enzyme activity. One unit (U) of enzyme activity corresponds to the conversion of 1 μmole of sucrose (used for hydrolysis and transglycosylation) under these conditions.

HPLC analysis was carried out on an Agilent MetaCarb 67H column (300 × 6.5 mm) with 2.5 mM H_2SO_4 as eluent under isocratic conditions and RI detection. The flow rate and temperature were set at 0.8 ml/min and 35 °C, respectively. Calibration of the obtained peaks was accomplished using the standard curves of sucrose, glucose and fructose.

2.4. Design of response surface methodology experiment

The response surface methodology (RSM) was applied to optimize the Gtf180-ΔN-Q1140E-catalyzed α-glucosylation of stevioside (acceptor substrate) with sucrose (donor substrate), while minimizing the synthesis of α-gluco-oligo/polysaccharides. All experiments were performed in 25 mM sodium acetate (pH 4.7), containing 1 mM $CaCl_2$, at 37 °C. The addition of 10 U/ml of enzyme ensured that a steady-state was reached within 3 h of incubation. A Box-Behnken design was generated, implementing stevioside concentration (mM), sucrose/stevioside ratio (D/A ratio) and agitation rate (rpm) as factors. For each of them, low (−1) and high (+1) level values were assigned as follows: stevioside concentration, (25 mM) and (100 mM); D/A ratio, (1) and (20); agitation rate, (0 rpm) and (200 rpm). The experimental design was generated and analyzed using JMP software (JMP®, Version 12. SAS Institute Inc., Cary, NC, 1989–2007) and consisted of 15 experiments carried out at a 5 ml scale (Supplementary Information, Table S1). The response surface analysis module of JMP software was applied to fit the following second order polynomial equation:

$$\hat{Y} = \beta_0 + \sum_{i=1}^{I} \beta_i X_i + \sum_{i=1}^{I} \beta_{ii} X_i^2 + \sum_i \sum_j \beta_{ij} X_i X_j$$

where $\hat{Y}$ is the predicted response, I is the number of factors (3 in this study), β_0 is the model constant, β_i is the linear coefficient associated with factor X_i, β_{ii} is the quadratic coefficient associated with factor X_i^2 and β_{ij} is the interaction coefficient between factors X_i and X_j. X_i represents the factor variable in coded form:

$$X_{c,i} = \frac{[X_i - (low + high)/2]}{(high - low)/2}$$

with $1 \leqslant i \leqslant I$, where $X_{c,i}$ is the coded variable.

For the HPLC analysis of steviol glycosides, an Agilent ZORBAX Eclipse Plus C18 column (100 × 4.6 mm, 3.5 μm) was used with water (solvent A) and acetonitrile (solvent B) as the mobile phases. The flow rate and temperature were set at 1.0 ml/min and 40 °C, respectively. The used gradient elution comprised 5–95% solvent B (0–25 min), 95% solvent B (25–27 min), 95–5% solvent B (27–30 min) and 5% solvent B (30–35 min). Detection was achieved with an ELS detector (evaporation temperature, 90 °C; nebulization temperature, 70 °C; gas flow rate, 1.6

SLM). Calibration of obtained Stev and mono-α-glucosylated Stev (Stev-G1) peaks was accomplished using standard curves of Stev and Stev-G1.

2.5. Preparation and isolation of α-glucosylated Stev products

The production of α-glucosylated Stev products was performed at a 50 ml scale in a shaker flask, by incubating 31 mM Stev and 524 mM sucrose with 10 U/ml of Gtf180-ΔN-Q1140E enzyme in 25 mM sodium acetate (pH 4.7), containing 1 mM $CaCl_2$, for 3 h at 37 °C. To isolate (α-glucosylated) Stev, separated from enzyme, remaining sucrose and side products glucose, fructose and gluco-oligo/polysaccharides, 10 ml portions were mixed with 4 g of hydrophobic resin Lewatit® VP OC 1064 MD PH (Lanxess, Antwerp, Belgium). After shaking for 30 min at 30 °C, the resin was collected and washed 3 times with 10 ml of distilled water, after which (α-glucosylated) Stev (Stev-G) was eluted from the resin by adding 20 ml of 70% ethanol. This product was used for the sensory analysis. For the isolation and structural analysis of α-glucosylated Stev components, Stev-G was fractionated by flash chromatography on a Reveleris X2 flash-chromatography system, equipped with a Reveleris Amino cartridge (40 g, 40 μm; Büchi Labortechnik GmbH, Hendrik-Ido-Ambacht, The Netherlands), using water (solvent A) and acetonitrile (solvent B) as the mobile phases (40 ml/min). The following gradient elution was used: 95% solvent B (0–2 column volumes (CV)), 95–50% solvent B (2–35 CV) and 50% solvent B (35–50 CV). Detection was achieved with UV (210 nm) and evaporative light scattering (ELS). The collected fractions Stev-G1 – Stev-G3 were evaporated *in vacuo* and subsequently lyophilized to remove the residual water.

The purity of Stev-G1 – Stev-G3 was checked by HPLC (UltiMate 3000 HPLC system; ThermoFisher Scientific, Amsterdam, The Netherlands) on a Luna 10 μm NH_2 column (250 × 4.6 mm; Phenomenex, Utrecht, The Netherlands) with acetonitrile (solvent A) and water, containing 0.025% acetic acid, (solvent B) as the mobile phases (1 ml/min). The following gradient elution was used: 80% solvent A (0–2 min), 80–50% solvent A (2–32 min), and a final washing step of 5 min at 20% solvent A. Detection was achieved with a VWD-3000 UV–vis detector at 210 nm (ThermoFisher Scientific). Stev-G1 turned out to be pure, whereas Stev-G2 and Stev-G3 needed further purification. Stev-G2 was purified on the Luna NH_2 column and Stev-G3 was subjected to further fractionation by high-pH anion-exchange chromatography (HPAEC). To this end, a Dionex DX500 workstation (Dionex, Amsterdam, The Netherlands), equipped with a CarboPac PA-1 column (250 × 9 mm; Dionex) and an ED40 pulsed amperometric detector, was used. The elution was performed at a flow rate of 3 ml/min with 10 mM NaOAc in 100 mM NaOH (8 min), followed by a 50 min gradient of 10 mM NaOAc to 13 mM NaOAc in 100 mM NaOH, a final washing step of 5 min at 100 mM NaOAc in 100 mM NaOH, and a 5 min equilibration step of 10 mM NaOAc in 100 mM NaOH. Collected fractions were immediately neutralized with 4 M acetic acid, desalted by solid-phase extraction (SPE) on Strata-X 33μ Polymeric Reversed Phase columns (Phenomenex). Briefly, the SPE columns were conditioned with 6 bed volumes (BV) of methanol and subsequently equilibrated with 6 BV de-ionized water. After loading the samples, the columns were washed with 6 BV de-ionized water, and the products were eluted with 6 BV 50% acetonitrile.

2.6. Analysis of site-specific α-glucosylation in Stev-G3

Fraction Stev-G3, isolated by flash-chromatography, was subjected to alkaline hydrolysis to release the carbohydrate moiety linked to the steviol C-19 carboxyl group, and leaving the carbohydrate moiety on the C-13 site intact (Gerwig, te Poele, Dijkhuizen, & Kamerling, 2017). Briefly, after treatment with 1.0 M NaOH at 80 °C for 2.5 h, cooling, and neutralization with 6 M HCl, the sample was desalted on a Strata-X PRP column (see above), evaporated to dryness, and investigated by NMR spectroscopy.

2.7. Methylation analysis

Steviol glycoside samples were permethylated using CH_3I and solid NaOH in $(CH_3)_2SO$, as described by Ciucanu and Kerek (1984), then hydrolyzed with 2 M trifluoroacetic acid (2 h, 120 °C) to give a mixture of partially methylated monosaccharides. After evaporation to dryness, the mixture was dissolved in H_2O and reduced with $NaBD_4$ (2 h, room temperature). Subsequently, the solution was neutralized with 4 M acetic acid and boric acid was removed by repeated co-evaporation with methanol. The obtained partially methylated alditol samples were acetylated with 1:1 acetic anhydride-pyridine (30 min, 120 °C). After evaporation to dryness, the mixtures of partially methylated alditol acetates were dissolved in dichloromethane and analyzed by GLC-EI-MS on an EC-1 column (30 m × 0.25 mm; Alltech/Grace, Deerfield, IL), using a GCMS-QP2010 Plus instrument (Shimadzu Kratos Inc., Manchester, UK) and a temperature gradient (140–250 °C at 8 °C/min) (Kamerling & Gerwig, 2007).

2.8. Mass spectrometry

Matrix-assisted laser desorption ionization time-of-flight mass spectrometry (MALDI-TOF-MS) was performed on an Axima™ mass spectrometer (Shimadzu Kratos Inc.), equipped with a nitrogen laser (337 nm, 3 ns pulse width). Positive-ion mode spectra were recorded using the reflector mode at a resolution of 5000 FWHM and delayed extraction (450 ns). Accelerating voltage was 19 kV with a grid voltage of 75.2%. The mirror voltage ratio was 1.12 and the acquisition mass range was 200–6000 Da. Samples were prepared by mixing on the target 1 μl sample solution with 1 μl of aqueous 10% 2,5-dihydroxybenzoic acid in 70% acetonitrile as matrix solution.

2.9. NMR spectroscopy

Resolution-enhanced 1D/2D 500-MHz $^1H/^{13}C$ NMR spectra were recorded in D_2O on a Bruker DRX-500 spectrometer (Bijvoet Center, Department of NMR Spectroscopy, Utrecht University). To avoid overlap of anomeric signals with the HOD signal, the 1D and 2D spectra were run at 310 K. Data acquisition was done with Bruker Topspin 2.1. Before analysis, samples were exchanged twice in D_2O (99.9 atom% D, Cambridge Isotope Laboratories, Inc., Andover, MA) with intermediate lyophilization, and then dissolved in 0.6 ml of D_2O. Fresh solutions (pD 7) of ~ 4 mg/ml were used for all NMR measurements. Suppression of the HOD signal was achieved by applying a WEFT (water eliminated Fourier transform) pulse sequence for 1D NMR experiments and by a pre-saturation of 1 s during the relaxation delay in 2D experiments. The 2D TOCSY spectra were recorded using an MLEV-17 [composite pulse devised by Levitt, Freeman, and Frenkiel (1982)] mixing sequence with spin-lock times of 20, 50, 100 and 200 ms. The 2D ^1H–^1H ROESY spectra were recorded using standard Bruker XWINNMR software with a mixing time of 200 ms. The carrier frequency was set at the downfield edge of the spectrum in order to minimize TOCSY transfer during spin-locking. Natural abundance 2D ^{13}C–^1H HSQC experiments (^1H frequency 500.0821 MHz, ^{13}C frequency 125.7552 MHz) were recorded without decoupling during acquisition of the ^1H FID. The NMR data were processed using the MestReNova 9 program (Mestrelab Research SL, Santiago de Compostella, Spain). Chemical shifts (δ) are expressed in ppm by reference to internal acetone (δ_H 2.225 for ^1H and δ_C 31.07 for ^{13}C).

2.10. Sensory analysis

Sensory analysis was performed in individual tasting booths at the UGent Sensolab (Belgium) by a trained panel (7 persons), as described previously by te Poele et al. (2018). In short, taste (sweetness, liquorice, astringency and bitterness) was evaluated by swirling the sample in the mouth for 5 s, after which the sample was expectorated. Aftertaste was

evaluated 10 s after swallowing the solution. Lingering, based on the maximum taste intensity, was rated 1 min later. Sucrose reference solutions (5%, 7.5% and 10% sucrose, scoring 5, 7.5 and 10, respectively) were provided. Water (Spa Reine) and plain crackers were used as palate cleansers between samplings. All samples were evaluated in duplicate.

Statistical analyses were performed with SPSS 23 (SPSS Inc., Chicago, USA). All tests were done at a significance level of 0.05. One-Way ANOVA was used to investigate any significant difference between the solutions. Testing for equal variances was executed with the Modified Levene Test. When conditions for equal variance were fulfilled, the Tukey test (Tukey, 1953) was used to determine differences between samples. In case variances were not equal, Games-Howell (Games & Howell, 1976) assay was performed.

Three different solutions sweetened with Stev products were examined: 588 mg/l of mono-α-glucosylated product (Stev-G1), 588 mg/l of multi-α-glucosylated product, containing residual Stev, Stev-G1 and higher α-glucosylated Stev (Stev-G), and twice the amount of Stev-G (1176 mg/l, denoted as Stev-G').

3. Results

3.1. Trans-α-glucosylation of stevioside with Gtf180-ΔN-Q1140E enzyme

The *Lactobacillus reuteri* wild-type glucansucrase Gtf180-ΔN and its derived Gtf180-ΔN-Q1140E mutant enzyme both readily catalyzed the trans-α-glucosylation of stevioside (Stev), using sucrose as donor substrate. However, in terms of percentage conversion to α-glucosylated Stev, the mutant enzyme is preferred over the wild-type (see below). As an example, Fig. 1 presents a typical HPLC profile of the resulting mixture (Stev-G) of an incubation of Stev, sucrose and the mutant enzyme.

As previously reported (te Poele et al., 2018), the optimization of the reaction conditions for trans-α-glucosylation of rebaudioside A (RebA) with Gtf180-ΔN-Q1140E revealed the importance of selecting adequate concentrations of donor substrate sucrose and acceptor substrate RebA. The addition of too much sucrose resulted in suboptimal yields due to increased α-gluco-oligo/polysaccharide synthesis. The glucosylation of Stev was therefore also optimized by response surface methodology (RSM), using a Box-Behnken experimental design. The following factors were considered: X_1, Stev concentration (mM); X_2, the

ratio of donor substrate sucrose over acceptor substrate Stev (D/A ratio); X_3, agitation speed (rpm). The addition of 10 U/ml of enzyme ensured that a steady state in Stev conversion was obtained within 3 h. The results of the Box-Behnken experimental design are summarized in Supplementary Information, Table S1. The analysis of variance (ANOVA) showed R^2 values of 98.8% and 98.7% for the Stev conversion degree (%) and the amount of α-glucosylated Stev (Stev-G) synthesized (mM), respectively. The effects of the factors were analyzed after applying the response surface contour plots (Fig. 2).

Higher Stev conversion degrees were obtained at decreasing Stev concentrations, independent on the concentration of the donor substrate sucrose. The effect of the D/A ratio on Stev conversion degrees displayed a distinct optimum. An increase in D/A ratio initially resulted in improved Stev conversion degrees, indicating that sucrose drives the reaction. However, as sucrose also acts as primer for α-gluco-oligo/polysaccharide synthesis (being the "natural" activity of glucansucrase), a further increase in D/A ratio resulted in less Stev glucosylation in favour of more α-gluco-oligo/polysaccharide synthesis. The concentrations of sucrose and Stev thus need to be carefully optimized. In contrast, the effect of agitation on Stev conversion degrees and the amount of Stev-G synthesized was negligible.

The resulting model was used for the optimization of the reaction conditions. An efficient conversion of Stev (at least 95%), yielding a maximal amount of Stev-G, was targeted. The model predicted the synthesis of 29 mM Stev-G in case the following conditions were applied: 31 mM Stev, 524 mM sucrose (D/A ratio of 16.9) and 0 rpm. The validation test resulted in the synthesis of 28 mM Stev-G (Supplementary Information, Fig. S1A), which was in good agreement with the prediction. Compared to the RebA α-glucosylation with Gtf180-ΔN-Q1140E (te Poele et al., 2018), much more donor substrate sucrose was needed to completely convert Stev (D/A ratio of 16.9 compared to 3.4), whereas less α-glucosylated product could be obtained (28 mM Stev-G vs. 80 mM RebA-G), indicating that the enzyme had a lower affinity for Stev than for RebA. Equally remarkable was that while RebA was mainly converted into mono-α-glucosylated product (RebA-G1, 77.7%), Stev was converted for only 32.5% into mono-α-glucosylated product (Stev-G1). Applying the optimal conditions for the α-glucosylation of Stev with wild-type Gtf180-ΔN resulted in the conversion of only 60.9% Stev with a Stev-G1/Stev-G ratio of 23.7% (Supplementary Information, Fig. S1B).

3.2. Structural characterization of α-glucosylated stevioside products

3.2.1. General

A large-scale 3 h incubation of 31 mM Stev and 524 mM sucrose with 10 U/ml of Gtf180-ΔN-Q1140E mutant enzyme at 37 °C (optimal RSM conditions) resulted in a final mixture containing residual sucrose, glucose, fructose, enzyme, gluco-oligo/polysaccharides and residual Stev + α-glucosylated Stev products (Stev-G). Flash-chromatography of the mixture made the isolation of three Stev-G fractions possible, namely Stev-G1, Stev-G2 and Stev-G3 (Supplementary Information, Fig. S2; compare with Fig. 1). MALDI-TOF-MS analysis of Stev-G, generated from a small-scale incubation and separated from enzyme, glucose, fructose, gluco-oligo/polysaccharides and residual sucrose by SPE (Strata–X PRP column), showed, besides steviolbioside (SB) (*m/z* 665.6) and residual Stev (*m/z* 827.6), a series of quasi-molecular ions [M + Na]$^+$, in accordance with an extension of Stev with one (Stev-G1; *m/z* 989.7), two (Stev-G2; *m/z* 1152.0), and up to nine (*m/z* 2287.8) glucose residues (Supplementary Information, Fig. S3B). It should be noted that a quasi-molecular ion [M + Na]$^+$ peak can reflect possibly several compounds with isomeric structures, due to position and linkage type of the attached glucose units. Fractions Stev-G1 – Stev-G3, isolated via flash-chromatography, turned out to be suitable for further analysis by a combination of 1D and 2D NMR spectroscopy, methylation analysis and mass spectrometry.
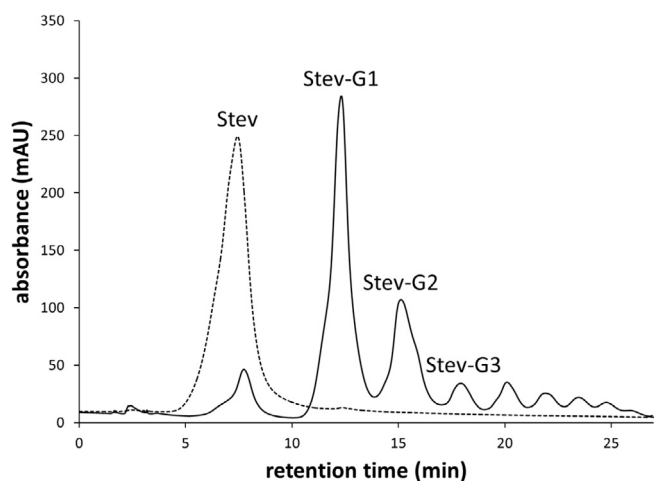

Fig. 1. HPLC fractionation pattern on a Luna 10 μm NH₂ column of (α-glucosylated) stevioside Stev-G after an incubation of 25 mM Stev, 500 mM sucrose with 10 U/ml Gtf180-ΔN-Q1140E mutant enzyme at t = 0 h (........) and t = 3 h (——). Enzyme, glucose, fructose, gluco-oligo/polysaccharides and residual sucrose were first removed by SPE. The profile after 27 min is deleted, because no further peaks were observed.
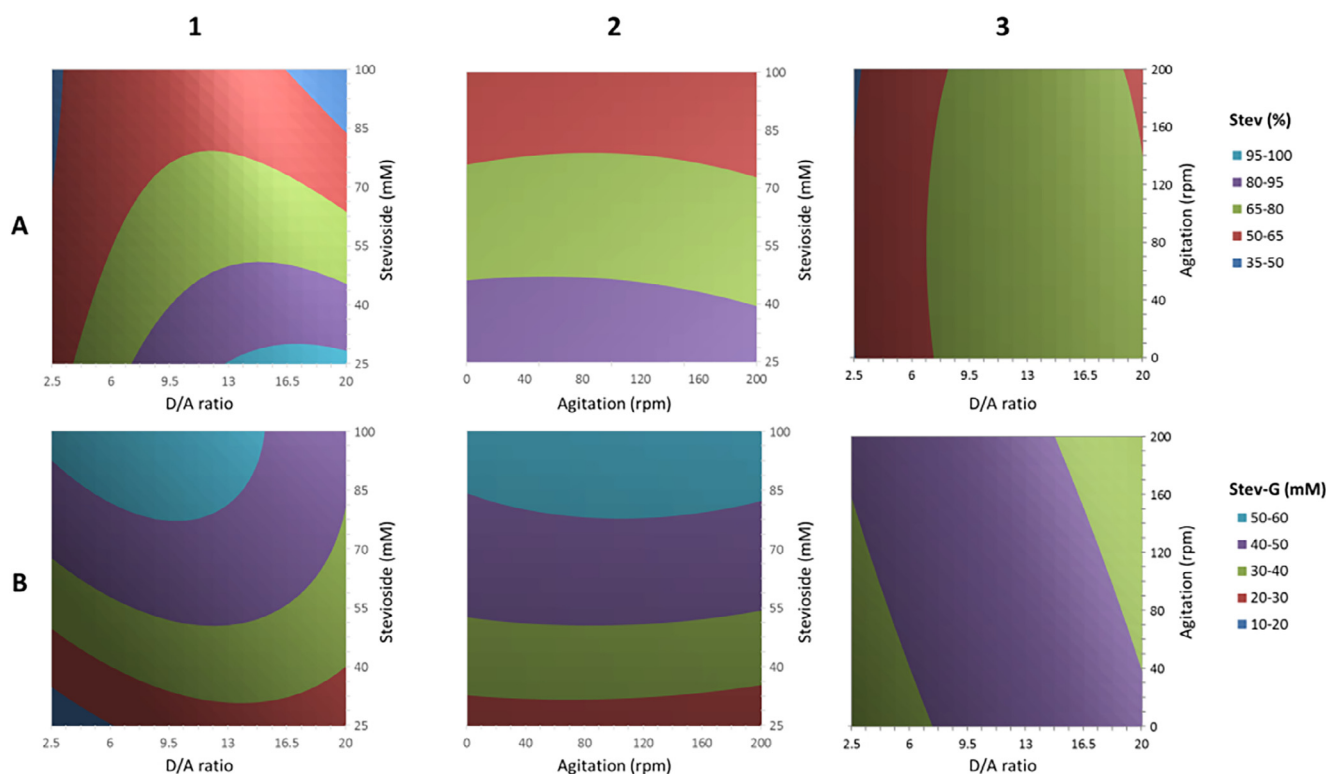
Fig. 2. Response surface methodology contour plots of stevioside (Stev) α-glucosylation by Gtf180-ΔN-Q1140E, showing the effects of: Stev concentration (mM); D/A ratio (ratio of donor substrate sucrose over acceptor substrate Stev); agitation (rpm) on: (A) Stev conversion degree (%); (B) Stev-G synthesized (mM).

3.2.2. Fraction Stev-G1

HPLC analysis on Luna NH_2 gave rise to a single peak for fraction Stev-G1. MALDI-TOF-MS analysis showed a quasi-molecular ion $[M + Na]^+$ at m/z 989.7, corresponding to Stev + 1Glc (Supplementary Information, Fig. S3C). Methylation analysis (Supplementary Information, Table S2) of Stev-G1 revealed terminal Glcp, 2-substituted Glcp and 6-substituted Glcp (molar ratio 2:1:1). When compared with the methylation analysis of Stev (Supplementary Information, Table S2), showing terminal Glcp and 2-substituted Glcp (molar ratio 2:1), the transglucosylation had resulted in elongation, not branching. The ^{1}H NMR spectrum of Stev-G1 (Fig. 3B) showed resonances of one dominant α-glucosylated Stev product. A slight contamination (< 10%) of the main product is reflected by the presence of five small signals (denoted with *: δ_H 5.35, 4.45, 4.14, 3.98, 3.16 in Fig. 3B). The spectrum between 0.8 and 2.2 ppm represents the typical steviol core signal pattern as seen for Stev (Fig. 3A). Besides the three β-anomeric ^{1}H signals related to Stev (**Glc1**, δ_H 5.415; **Glc2**, δ_H 4.725; **Glc3**, δ_H 4.675), one extra anomeric ^{1}H resonance (δ_H 4.862; $J_{1,2}$ 3.7 Hz), partially overlapping with one steviol C-17 proton, was observed, stemming from a new α-linked Glc residue (**Glc4**). Using 2D NMR spectroscopy (TOCSY with different mixing times, ROESY, HSQC) (Supplementary Information, Figs. S4 and S6), the ^{1}H/^{13}C chemical shifts of the steviol core (Supplementary Information, Table S3) and the four Glc residues (Table 1) of Stev-G1 (main component) were assigned, and a **Glc4**(α1 → 6)**Glc1** element could be established (van Leeuwen, Leeflang, Gerwig, & Kamerling, 2008; Gerwig et al., 2017). Based on the various analytical data, the conclusive structure of the main component in fraction Stev-G1 is Stev elongated with a Glc(α1 → 6) residue at the Glc(β1 → C-19 site of the steviol core (Fig. 4).
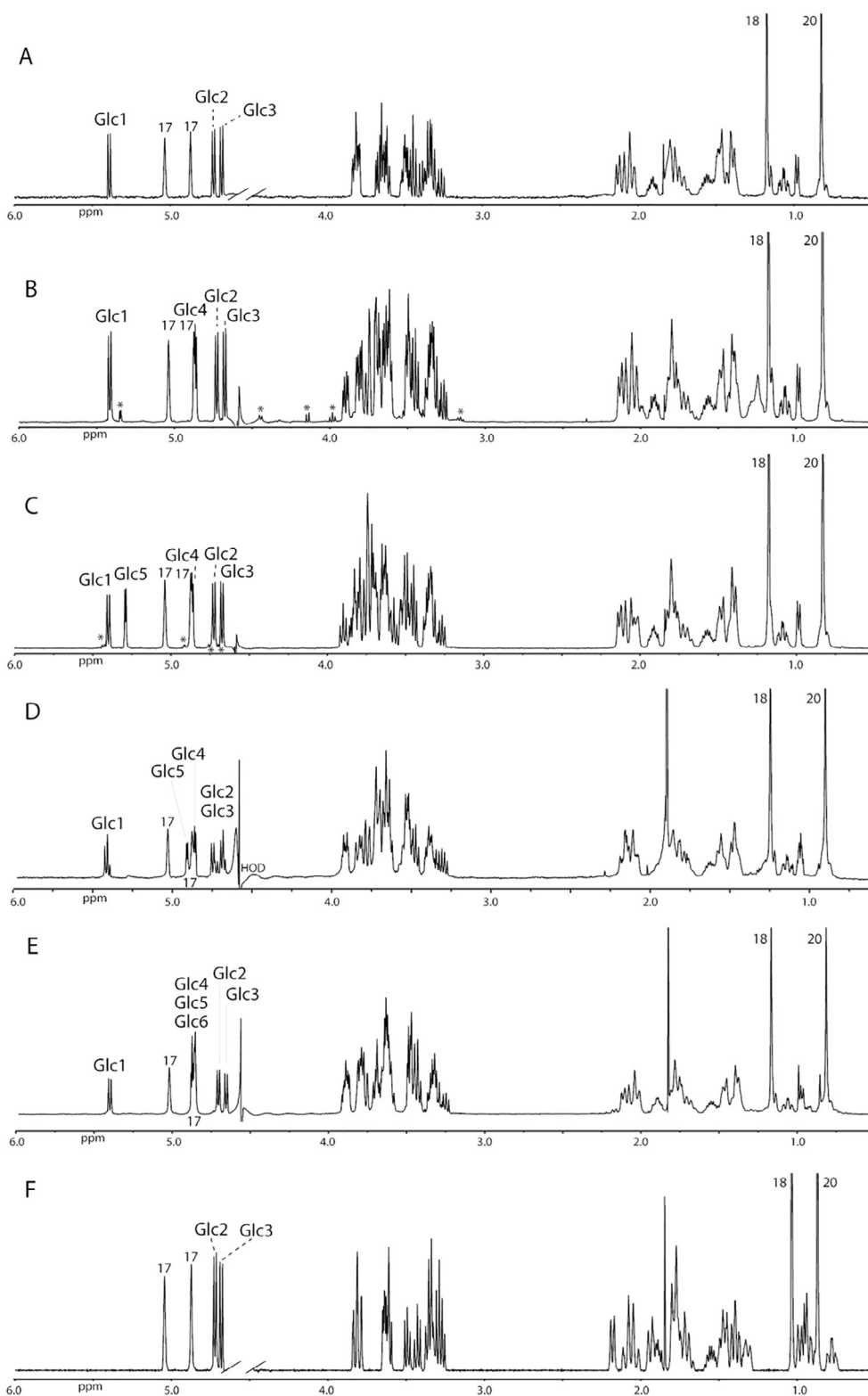
3.2.3. Fraction Stev-G2

As HPLC analysis on Luna NH_2 did not reveal a single peak for fraction Stev-G2, an additional purification step on the same column material was carried out. MALDI-TOF-MS analysis of purified Stev-G2 showed a quasi-molecular ion $[M + Na]^+$ at m/z 1152.0, corresponding to Stev + 2Glc (Supplementary Information, Fig. S3D). Methylation analysis (Supplementary Information, Table S2) of Stev-G2 showed terminal Glcp, 2-substituted Glcp, 4-substituted Glcp and 6-substituted Glcp (molar ratio 2:1:1:1), together with a trace amount (< 2%) of 2,6-disubstituted Glcp. The ^{1}H NMR spectrum of Stev-G2 (Fig. 3C) exhibited the typical steviol core signal pattern as seen for Stev (Fig. 3A). Besides the three β-anomeric ^{1}H carbohydrate signals related to Stev (**Glc1**, δ_H 5.415; **Glc2**, δ_H 4.727; **Glc3**, δ_H 4.674), two α-anomeric ^{1}H resonances of equal intensity (δ_H 4.863, $J_{1,2}$ 3.9 Hz and δ_H 5.292, $J_{1,2}$ 3.7 Hz) were observed, stemming from two new α-linked Glc residues (**Glc4** and **Glc5**). The ^{1}H NMR spectrum indicated the presence of one main di-α-glucosylated Stev product, together with very minor products/contaminants (< 10%), represented by four small anomeric signals (indicated with *: δ_H 5.43, 4.91, 4.75, 4.71 in Fig. 3C). Using 2D NMR spectroscopy (TOCSY with different mixing times, ROESY, HSQC) (Supplementary Information, Figs. S7 and S8), the ^{1}H/^{13}C chemical shifts of the steviol core (Supplementary Information, Table S3) and the five Glc residues (Table 1) of Stev-G2 (main component) were assigned (van Leeuwen, et al., 2008; Gerwig, et al., 2017). Based on the various analytical data, the conclusive structure of the main component in fraction Stev-G2 is Stev elongated with a Glc(α1 → 4)Glc(α1 → 6) element at the Glc(β1 → C-19 site of the steviol core (Fig. 4).

3.2.4. Fraction Stev-G3

MALDI-TOF-MS analysis of fraction Stev-G3 showed mainly $[M + Na]^+$ peaks for SB (m/z 665.5), Stev + 3Glc (m/z 1314.2) and Stev + 4Glc (m/z 1475.6) (Supplementary Information, Fig. S3E). Methylation analysis revealed the presence of terminal Glcp, 2-substituted Glcp, 3-substituted Glcp, 4-substituted Glcp, 6-substituted Glcp and 2,6-disubstituted Glcp in a ratio that suggests the presence of a complex mixture (Supplementary Information, Table S2). Moreover, inspection of the 1D and 2D NMR data of Stev-G3 confirmed the complexity, and suggested that, next to the α-glucosylation at **Glc1** of the steviol C-19

Fig. 3. 500-MHz ^{1}H NMR spectra of reference Stev (**A**) and α-glucosylated fractions Stev-G1 (**B**), Stev-G2 (**C**), Stev-G3.1 (**D**), Stev-G3.4 (**E**) and steviolbioside (**F**), recorded in D$_2$O at 310 K. * Resonances stemming from additional minor product(s). Note that the two H-17 protons (C = CH$_2$) of the steviol core appear as broad singlets, due to a very small geminal coupling.

site, **Glc2** and/or **Glc3** of the β-sophorosyl disaccharide at the steviol C-13 site might contain α-Glc*p* substitutions (data not shown).

To get further information about the suspected presence of α-glucosylation on the steviol C-13 site, an alkaline treatment of fraction Stev-G3 was performed (Gerwig, et al., 2017). The specific cleavage of

the carboxyl-glucosylated ester linkage, leaving the steviol C-13 part intact, would produce only steviolbioside (SB) in case of the absence of modification at the C-13 site. NMR analysis (including TOCSY, ROESY and HSQC) of the product mixture after alkaline treatment, isolated by SPE, showed that **Glc1** (with elongations) had indeed disappeared but

Table 1

¹H and ¹³C chemical shifts (δ)[a] for the Glcp residues of stevioside (Stev), the α-glucosylated Stev products from fractions Stev-G1 (Stev + 1Glc), Stev-G2 (Stev + 2Glc), Stev-G3.1 (Stev + 2Glc) and Stev-G3.4 (Stev + 3Glc), and steviolbioside (SB), recorded in D₂O at 310 K. For structures, see Fig. 4.

Residue	Stev		Stev-G1		Stev-G2		Stev-G3.1		Stev-G3.4		SB	
	¹H	¹³C	¹H	¹³C	¹H	¹³C	¹H	¹³C	¹H	¹³C	¹H	¹³C
Glc1(β1 → C-19)												
H-1	5.397	95.4	5.415	95.5	5.415	95.4	5.429	95.5	5.421	95.5	–	–
H-2	3.46	73.6	3.46	73.0	3.45	73.4	3.46	73.0	3.45	73.4	–	–
H-3	3.50	78.0	3.50	77.8	3.50	77.9	3.51	77.5	3.50	77.7	–	–
H-4	3.40	70.7	3.45	70.6	3.45	70.6	3.46	70.8	3.45	70.8	–	–
H-5	3.50	77.7	3.70	77.0	3.70	76.9	3.70	76.8	3.71	77.0	–	–
H-6a	3.82	62.2	3.89	*66.7*[b]	3.85	*67.4*	3.90	*66.7*	3.90	*67.0*	–	–
H-6b	3.67		3.70		3.74		3.71		3.75		–	
Glc2(β 1 → C-13)												
H-1	4.726	97.2	4.725	97.3	4.727	97.2	4.737	97.2	4.725	97.3	4.724	97.5
H-2	3.49	*82.2*	3.49	*82.2*	3.49	*82.1*	3.51	*81.5*	3.49	*82.2*	3.49	*81.9*
H-3	3.62	77.6	3.62	77.7	3.62	77.6	3.62	77.4	3.62	77.7	3.61	78.0
H-4	3.34	71.2	3.34	71.1	3.35	71.0	3.50	70.7	3.35	71.3	3.35	71.4
H-5	3.33	77.2	3.34	77.4	3.34	77.2	3.54	75.8	3.34	77.3	3.34	77.6
H-6a	3.80	62.2	3.80	62.2	3.80	62.2	3.91	*66.9*	3.81	62.4	3.80	62.6
H-6b	3.63		3.63		3.65		3.64		3.64		3.63	
Glc3(β 1 → 2)												
H-1	4.675	104.3	4.675	104.5	4.674	104.4	4.689	104.4	4.675	104.4	4.685	104.5
H-2	3.26	75.7	3.27	75.8	3.27	75.8	3.27	75.7	3.27	75.5	3.27	75.9
H-3	3.45	77.0	3.45	77.3	3.45	77.0	3.45	77.0	3.45	77.1	3.43	77.4
H-4	3.32	71.2	3.34	71.1	3.33	71.2	3.32	71.1	3.34	71.3	3.29	71.6
H-5	3.35	77.4	3.34	77.4	3.35	77.2	3.36	77.5	3.36	77.5	3.35	78.0
H-6a	3.82	62.2	3.82	62.2	3.82	62.2	3.82	62.3	3.82	62.4	3.83	62.6
H-6b	3.64		3.64		3.64		3.64		3.64		3.63	
Glc4			**(α1→6)Glc1**		**(α 1 → 6)Glc1**		**(α 1 → 6)Glc1**		**(α 1 → 6)Glc1**			
H-1	–	–	4.862	99.3	4.862	99.2	4.864	99.2	4.876	99.2	–	–
H-2	–	–	3.48	73.0	3.53	72.9	3.48	73.1	3.49	72.8	–	–
H-3	–	–	3.65	74.4	3.90	74.8	3.65	73.9	3.66	74.0	–	–
H-4	–	–	3.36	71.3	3.58	*77.9*	3.37	70.9	3.42	71.2	–	–
H-5	–	–	3.62	73.5	3.70	71.7	3.68	73.4	3.86	72.1	–	–
H-6a	–	–	3.75	62.0	3.75	61.8	3.77	62.0	3.91	*67.5*	–	–
H-6b	–		3.68		3.70		3.68		3.66		–	
Glc5					**(α 1 → 4)Glc4**		**(α 1 → 6)Glc2**		**(α 1 → 6)Glc4**			
H-1	–	–	–	–	5.292	101.6	4.912	94.2	4.882	99.4	–	–
H-2	–	–	–	–	3.52	73.1	3.51	72.7	3.51	72.8	–	–
H-3	–	–	–	–	3.63	74.3	3.67	74.4	3.66	74.0	–	–
H-4	–	–	–	–	3.37	71.0	3.38	70.9	3.48	71.2	–	–
H-5	–	–	–	–	3.64	74.3	3.66	73.5	3.86	72.0	–	–
H-6a	–	–	–	–	3.78	61.8	3.79	62.0	3.92	*67.1*	–	–
H-6b	–		–		3.70		3.69		3.72		–	
Glc6									**(α1→6)Glc5**			
H-1	–	–	–	–	–	–	–	–	4.875	99.5	–	–
H-2	–	–	–	–	–	–	–	–	3.48	73.1	–	–
H-3	–	–	–	–	–	–	–	–	3.65	74.7	–	–
H-4	–	–	–	–	–	–	–	–	3.36	71.3	–	–
H-5	–	–	–	–	–	–	–	–	3.64	73.5	–	–
H-6a	–	–	–	–	–	–	–	–	3.80	62.3	–	–
H-6b	–		–		–		–		3.69		–	

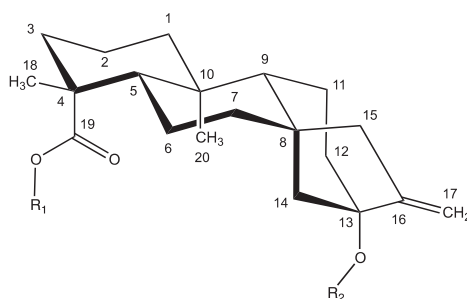[a] In ppm relative to the signal of internal acetone (δ 2.225 for ¹H and δ 31.07 for ¹³C).
[b] Substituted carbon positions are indicated in italics.

the presence of α-anomeric signals, together with deviations of proton chemical shifts (TOCSY) of **Glc2** and **Glc3**, compared to those in Stev, indicated Glc(α1 → 6) elongations on these residues, confirmed by HSQC (Supplementary Information, Fig. S9 and Table S4). However, it is not clear whether both substitutions are present together or individually. Moreover, it has to be noted that the majority of Stev-G3 was converted to steviolbioside (SB) by the alkaline treatment, indicating that α-glucosylation had occurred mainly at the steviol C-19 site. As positive control, the elimination of **Glc1** by a similar alkaline treatment of Stev resulted in steviolbioside (SB).

Fraction Stev-G3 was further subfractionated by high-pH anion-exchange chromatography (HPAEC) on CarboPac PA-1, yielding four subfractions, denoted Stev-G3.1, Stev-G3.2, Stev-G3.3 and Stev-G3.4

(Supplementary Information, Fig. S10). MALDI-TOF-MS analysis of Stev-G3.1 – Stev-G3.4 demonstrated that the individual subfractions are still mixtures. Stev-G3.1 (Supplementary Information, Fig. S3F) showed mainly peaks for Stev + 2Glc (*m/z* 1152.7) and Stev + 1Glc (*m/z* 989.6), there being minor peaks in the MS spectrum of Stev-G3 (Supplementary Information, Fig. S3E). Stev-G3.2 and Stev-G3.3 showed complex peak patterns (spectra not shown), whereas Stev-G3.4 (Supplementary Information, Fig. S3G) showed mainly SB (*m/z* 665.6) and Stev + 3Glc (*m/z* 1314.8). The origin of a peak for SB is not clear; probably it has an MS background (loss of ester-linked carbohydrate during acquisition), but could also be an artifact of the HPAEC protocol (release of ester-linked carbohydrate under basic conditions). The complexity of the fractions was confirmed by inspection of the

SB	R₁ = H		R₂ = β-D-Glc*p*-(1→2)-β-D-Glc*p*-(1→
			[Glc3] [Glc2]

The figure labels are laid out as follows:

Fig. 4. Structures of steviolbioside (SB), stevioside (Stev), and α-glucosylated Stev products [fractions Stev-G1 (main Stev + 1Glc), Stev-G2 (main Stev + 2Glc), Stev-G3.1 (main Stev + 2Glc) and Stev-G3.4 (main Stev + 3Glc)].

corresponding ¹H NMR spectra. Further investigations on Stev-G3.2 and Stev-G3.3 failed; therefore, attention will only be paid to fractions Stev-G3.1 and Stev-G3.4.

Methylation analysis of Stev-G3.1 (major [M + Na]⁺ MS-peak for Stev + 2Glc) showed terminal Glc*p*, 6-substituted Glc*p* and 2,6-disubstituted Glc*p* as major components, together with a smaller amount of 2-substituted Glc*p* (Supplementary Information, Table S2). Further analysis by 1D/2D ¹H/¹³C NMR spectroscopy (see Supplementary Information, Figs. S11 and S12) revealed that the structure of the major α-glucosylated product in Stev-G3.1 had a steviol core with a Glc(α1 → 4)Glc(β1 → disaccharide at the C-19 site and a Glc (β1 → 2)[Glc(α1 → 6)]Glc(β1 → trisaccharide at the C-13 site (Fig. 4). The Stev + 1Glc component, seen in the MALDI-TOF mass spectrum could be explained as a MS fragmentation or a HPAEC ester degradation.

Methylation analysis of Stev-G3.4 (major [M + Na]⁺ MS-peak for Stev + 3Glc) revealed terminal Glc*p*, 2-substituted Glc*p* and 6-substituted Glc*p* as major components, together with a minor amount of 2,6-disubstituted Glc*p* (Supplementary Information, Table S2). Further analysis by 1D/2D ¹H/¹³C NMR spectroscopy (see Supplementary Information, Figs. S13 and S14) revealed that the structure of the major α-glucosylated product in Stev-G3.4 had a steviol core with a Glc(α1 → 6)Glc(α1 → 6)Glc(α1 → 6)Glc(β1 → tetrasaccharide at the C-19 site and a Glc(β1 → 2)Glc(β1 → disaccharide at the C-13 site (Fig. 4). The peak for SB, seen in the mass spectrum, could be explained as a MS fragmentation of the C-19 ester linkage or ester degradation during HPAEC. In both cases the major Stev-G3.4 component is the precursor of SB. In view of the known Gtf180-ΔN glucansucrase enzyme activity, which mainly catalyzed the introduction of alternating (α1 → 3)/(α1 → 6) linkages, the successive (α1 → 6)-elongation at the Glc(β1 → C-19 site is remarkable. However, a minor successive (α1→6)-elongation at the Glc(β1 → C-19 site was also found during the trans-α-glucosylation of RebA with wild-type Gtf180-ΔN glucansucrase (Gerwig et al., 2017).

3.3. Sensory analysis of glucosylated stevioside products

A sensory analysis of aqueous solutions sweetened with Stev and several α-glucosylated Stev products was performed by a trained panel, evaluating nine different taste attributes. Three different product solutions were examined: 588 mg/l of mono-α-glucosylated product (Stev-G1), 588 mg/l of multi-α-glucosylated product (residual Stev, Stev-G1 and higher α-glucosylated Stev) (Stev-G) and 1176 mg/l of multi-α-glucosylated product (Stev-G'). The mean scores of the taste attributes of the sweetened solutions are shown in Fig. 5.

All α-glucosylated Stev products were significantly less bitter than stevioside. Stev-G1 retained the very high sweetness typical of steviol glycosides such as Stev. In contrast, Stev-G was significantly less sweet than Stev, which can be explained by the relatively large proportion of multi-α-glucosylated products. Multi-α-glucosylation resulted, not only in a further decrease of bitterness, but it simultaneously decreased sweetness as well. In addition, Stev-G was also significantly less liquorice and lingering than was Stev (Fig. 5). Doubling the concentration of Stev-G from 588 mg/l to 1176 mg/l (Stev-G') roughly resulted in a duplication of the sweetness, equaling the sweetness level of Stev, whereas bitterness and off-flavours were still equally suppressed. Glucosylation of stevioside with Gtf180-ΔN-Q1140E is thus a very adequate method to improve its sensory properties, i.e. by reducing the typical bitterness to a very low level.

4. Discussion

Although stevioside (Stev) is the most abundant of all steviol glycosides extracted from the leaves of the *Stevia rebaudiana* plant, its lingering bitterness prevents applications as a sweetener in low-calorie foods and beverages. All current *Stevia* food products are based on rebaudioside A (RebA), perceived as less bitter than Stev, implying that the latter is discarded as a "side product". In the present investigation, we have demonstrated that the α-glucosylation of Stev with sucrose as donor and the Gtf180-ΔN-Q1140E mutant enzyme as catalyst, offers a viable method for significantly reducing its bitterness, thereby improving the edulcorant/organoleptic properties. After optimization of the reaction conditions by RSM, a very high Stev conversion of 95%, yielding 50 g/l of Stev-G within 3 h, was obtained, while using only 10 U/ml of enzyme. Structural analysis of Stev-G components revealed that Stev was mostly mono-(α1 → 6)-glucosylated at the β-Glc residue of the steviol C-19 site (Stev-G1; Fig. 4). The minor components

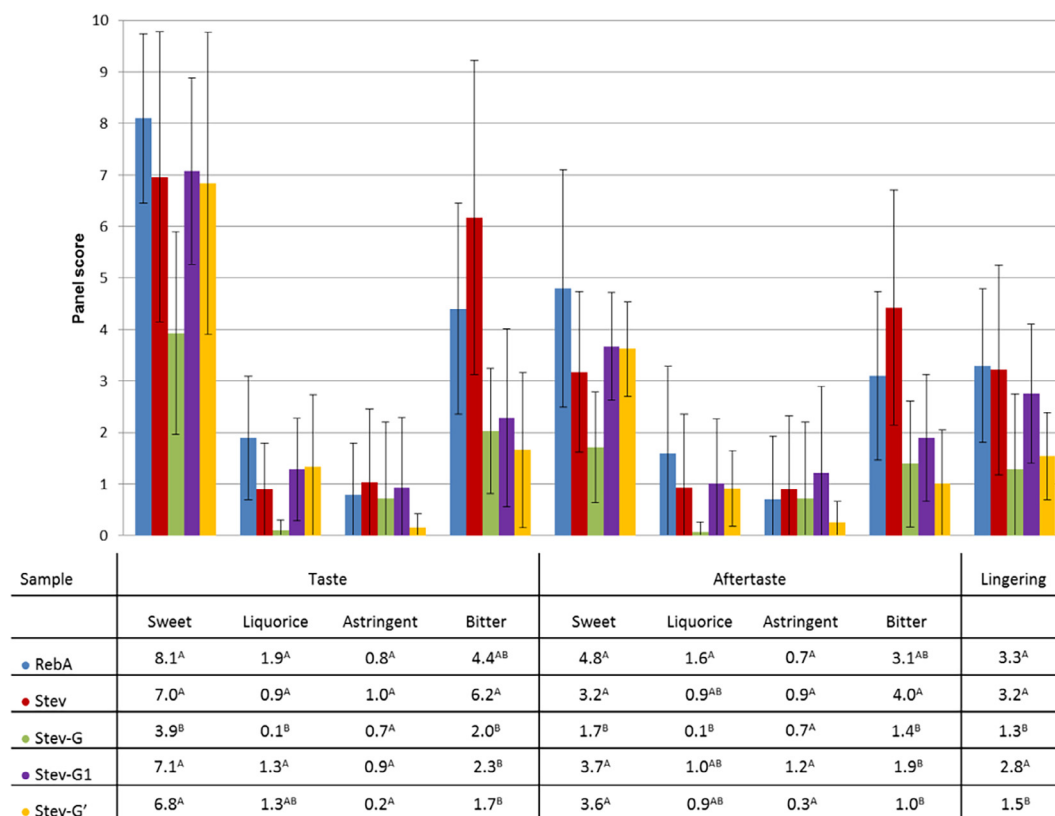| Sample	Taste				Aftertaste				Lingering
	Sweet	Liquorice	Astringent	Bitter	Sweet	Liquorice	Astringent	Bitter	
• RebA	8.1[A]	1.9[A]	0.8[A]	4.4[AB]	4.8[A]	1.6[A]	0.7[A]	3.1[AB]	3.3[A]
• Stev	7.0[A]	0.9[A]	1.0[A]	6.2[A]	3.2[A]	0.9[AB]	0.9[A]	4.0[A]	3.2[A]
• Stev-G	3.9[B]	0.1[B]	0.7[A]	2.0[B]	1.7[B]	0.1[B]	0.7[A]	1.4[B]	1.3[B]
• Stev-G1	7.1[A]	1.3[A]	0.9[A]	2.3[B]	3.7[A]	1.0[AB]	1.2[A]	1.9[B]	2.8[A]
• Stev-G'	6.8[A]	1.3[AB]	0.2[A]	1.7[B]	3.6[A]	0.9[AB]	0.3[A]	1.0[B]	1.5[B]

Fig. 5. Sensory analysis of stevioside (Stev), Stev-G, Stev-G1 and Stev-G'. [A,B]: different letters indicate significant differences ($p < 0.05$) between solutions following one-way ANOVA and *post-hoc* test.

represent a complex mixture of multi-α-glucosylated products (> 50% of Stev-G), whereby elongations at both the steviol C-19 and C-13 sites were found; see the established structures for Stev-G2, Stev-G3.1 and Stev-G3.4 (Fig. 4). Although Stev-G was perceived as half as sweet as Stev, probably due to the multi-α-glucosylation, this undesired effect could be compensated by doubling the dose of Stev-G (Stev-G'). Remarkably, this did not affect the significantly reduced perception of bitterness nor that of other off-flavours. Moreover, the increase of caloric content is negligible.

In the context of trans-α-glucosylation of steviol glycosides by glucansucrases, a recent study reported the application of a dextransucrase from *Leuconostoc citreum* KM20 for the α-glucosylation of Stev. Similarly to our results, the *L. citreum* dextransucrase glucosylated Stev at the C-19 site through an (α1 → 6)-linkage, alleviating its bitterness and off-flavours (Ko et al., 2016). A high conversion degree (94%) was obtained; however, much more enzyme (4500 U/ml vs. 10 U/ml) and a longer incubation time (5 days vs. 3 h) were needed. The volumetric productivity per U enzyme of the mutant Gtf180-ΔN-Q1140E enzyme reaction is consequently > 2000 times higher. Trans-α-glucosylation of Stev, using sucrose as donor substrate, was also achieved with an alternansucrase (EC 2.4.1.140) from *L. citreum* SK24.002, an enzyme that introduces (α1 → 6) and (α1 → 3) linkages (Musa, Miao, Zhang, & Jiang, 2014). Under optimized reaction conditions, a maximum conversion degree of only 44% was achieved. Stev was elongated at the terminal Glc(β1 → 2) residue of the β-sophorosyl unit at the steviol C-13 site with an (α1 → 6) linkage. Also a tri-α-glucosylated Stev was structurally characterized and was shown to contain an (α1 → 3)-(α1 → 6)-(α1 → 3) extension at the terminal Glc(β1 → 2) residue at the steviol C-13 site. A taste comparison of the products was not reported. In addition, a mono-α-glucosylated Stev product, containing a Glc (α1 → 6) residue at the steviol C-19-ester-linked Glc(β1 → residue (comparable with our Stev-G1), has been synthesized with β-amylase Biozyme L and maltose as glucose donor. This also led to an

improvement in quality of taste (Lobov, Kasai, Ohtani, & Yamasaki, 1991), as shown here for the Gtf180-ΔN-Q1140E products. Furthermore, the report indicated that synthesized products elongated at the steviol C-13 site had a decreased quality of taste.

The process of trans-α-glucosylation by a mutant glucansucrase from *L. reuteri* 180 described in our work is clearly superior to other glucansucrase-catalyzed Stev glucosylation reactions, by meeting three important requirements, namely an adequate product specificity (mainly mono-α-glucosylation at one steviol site), a complete Stev conversion and a high space–time yield.

Appendix A. Supplementary data

Supplementary data associated with this article can be found, in the online version, at https://doi.org/10.1016/j.foodchem.2018.08.025.

References

Abelyan, V., Balayan, A., Ghochikyan, V., & Markosyan, A. (2004). Transglycosylation of stevioside by cyclodextrin glucanotransferases of various groups of microorganisms. *Applied Biochemistry and Microbiology, 40,* 129–134.

Bearth, A., Cousin, M. E., & Siegrist, M. (2014). The consumer's perception of artificial food additives: Influences on acceptance, risk and benefit perceptions. *Food Quality and Preference, 38,* 14–23.

Calle, E. E., Rodriguez, C., Walker-Thurmond, K., & Thun, M. J. (2003). Overweight, obesity, and mortality from cancer in a prospectively studied cohort of US adults. *The New England Journal of Medicine, 348*, 1625–1638.

Ciucanu, I., & Kerek, F. (1984). A simple and rapid method for the permethylation of carbohydrates. *Carbohydrate Research, 131*, 209–217.

Colsoul, B., Schraenen, A., Lemaire, K., Quintens, R., Van Lommel, L., Segal, A., ... Vennekens, R. (2010). Loss of high-frequency glucose-induced Ca^{2+} oscillations in pancreatic islets correlates with impaired glucose tolerance in $Trpm5^{-/-}$ mice. *Proceedings of the National Academy of Science of the United States of America, 107*, 5208–5213.

Desmet, T., Soetaert, W., Bojarova, P., Kren, V., Dijkhuizen, L., Eastwick-Field, V., & Schiller, A. (2012). Enzymatic glycosylation of small molecules: Challenging substrates require tailored catalysts. *Chemistry – A European Journal, 18*, 10786–10801.

Devlamynck, T., te Poele, E. M., Meng, X., van Leeuwen, S. S., & Dijkhuizen, L. (2016). Glucansucrase Gtf180-ΔN of *Lactobacillus reuteri* 180: Enzyme and reaction engineering for improved glycosylation of non-carbohydrate molecules. *Applied Microbiology and Biotechnology, 100*, 7529–7539.

EU Commission (2011). Commission Regulation (EU) No. 1131/2011. *Official Journal of the European Union, L295*, 205–211.

Faus, I. (2000). Recent developments in the characterization and biotechnological production of sweet-tasting proteins. *Applied Microbiology and Biotechnology, 53*, 145–151.

Field, A. E., Coakley, E. H., Must, A., Spadano, J. L., Laird, N., Dietz, W. H., ... Colditz, G. A. (2001). Impact of overweight on the risk of developing common chronic diseases during a 10-year period. *Archives of Internal Medicine, 161*, 1581–1586.

Games, P., & Howell, J. (1976). Pairwise multiple comparison procedures with unequal N's and/or variances: A Monte Carlo study. *Journal of Educational Statistics, 1*, 113–125.

Gerwig, G. J., te Poele, E. M., Dijkhuizen, L., & Kamerling, J. P. (2016). *Stevia* glycosides: Chemical and enzymatic modifications of their carbohydrate moieties to improve the sweet-tasting quality. *Advances in Carbohydrate Chemistry and Biochemistry, 73*, 1–72.

Gerwig, G. J., te Poele, E. M., Dijkhuizen, L., & Kamerling, J. P. (2017). Structural analysis of rebaudioside A derivatives obtained by *Lactobacillus reuteri* 180 glucansucrase-catalyzed trans-α-glucosylation. *Carbohydrate Research, 440–441*, 51–62.

Goyal, S. K., Samsher, & Goyal, R. K (2010). Stevia (*Stevia rebaudiana*) a bio-sweetener: A review. *International Journal of Food Sciences and Nutrition, 61*, 1–10.

Gregg, E. W., Cheng, Y. J., Cadwell, B. L., Imperatore, G., Williams, D. E., Flegal, K. M., ... Williamson, D. F. (2005). Secular trends in cardiovascular disease risk factors according to body mass index in US adults. *The Journal of the American Medical Association, 293*, 1868–1874.

Hellfritsch, C., Brockhoff, A., Stähler, F., Meyerhof, W., & Hofmann, T. (2012). Human psychometric and taste receptor responses to steviol glycosides. *Journal of Agricultural and Food Chemistry, 60*, 6782–6793.

Kamerling, J. P., & Gerwig, G. J. (2007). Strategies for the structural analysis of carbohydrates. In J. P. Kamerling, G. J. Boons, Y. C. Lee, A. Suzuki, N. Taniguchi, & A. G. J. Voragen (Eds.). *Comprehensive Glycoscience - From Chemistry to Systems Biology* (pp. 1–68). Oxford: Elsevier Ltd.

Ko, J. A., Nam, S. H., Park, J. Y., Wee, Y., Kim, D., Lee, W. S., ... Kim, Y. M. (2016). Synthesis and characterization of glucosyl stevioside using *Leuconostoc* dextransucrase. *Food Chemistry, 211*, 577–582.

Kralj, S., van Geel-Schutten, I. G. H., Dondorff, M. M. G., Kirsanovs, S., van der Maarel, M. J. E. C., & Dijkhuizen, L. (2004). Glucan synthesis in the genus *Lactobacillus*: Isolation

and characterization of glucansucrase genes, enzymes and glucan products from six different strains. *Microbiology, 150*, 3681–3690.

Leemhuis, H., Pijning, T., Dobruchowska, J. M., van Leeuwen, S. S., Kralj, S., Dijkstra, B. W., & Dijkhuizen, L. (2013). Glucansucrases: Three-dimensional structures, reactions, mechanism, α-glucan analysis and their implications in biotechnology and food applications. *Journal of Biotechnology, 163*, 250–272.

Levitt, M. H., Freeman, R., & Frenkiel, T. (1982). Broad-band heteronuclear decoupling. *Journal of Magnetic Resonance, 47*, 328–330.

Liu, H. M., Sugimoto, N., Akiyama, T., & Maitani, T. (2000). Constituents and their sweetness of food additive enzymatically modified licorice extract. *Journal of Agricultural and Food Chemistry, 48*, 6044–6047.

Lobov, S. V., Kasai, R., Ohtani, K., & Yamasaki, K. (1991). Enzymic production of sweet stevioside derivatives: Transglucosylation by glucosidases. *Agricultural and Biological Chemistry, 55*, 2959–2965.

Murata, Y., Yoshikawa, S., Suzuki, Y. A., Sugiura, M., Inui, H., & Nakano, Y. (2006). Sweetness characteristics of the triterpene glycosides in *Siraitia grosvenori. Journal of the Japanese Society for Food Science and Technology, 53*, 527–533.

Musa, A., Miao, M., Zhang, T., & Jiang, B. (2014). Biotransformation of stevioside by *Leuconostoc citreum* SK24.002 alternansucrase acceptor reaction. *Food Chemistry, 146*, 23–29.

Philippaert, K., Pironet, A., Mesuere, M., Sones, W., Vermeiren, L., Kerselaers, S., ... Vennekens, R. (2017). Steviol glycosides enhance pancreatic beta-cell function and taste sensation by potentiation of TRPM5 channel activity. *Nature Communications, 8*, 14733.

Prawitt, D., Monteilh-Zoller, M. K., Brixel, L., Spangenberg, C., Zabel, B., Fleig, A., & Penner, R. (2003). TRPM5 is a transient Ca^{2+}-activated cation channel responding to rapid changes in $[Ca^{2+}]_i$. *Proceedings of the National Academy of Science of the United States of America, 100*, 15166–15171.

Sips, N. C. A. P., & Vercauteren, R. L. M. (2011). Sweetener compositions with reduced bitter off taste and methods of preparing. WO 2011143465.

Sun, Y. H. (2008). Health concern, food choice motives, and attitudes toward healthy eating: The mediating role of food choice motives. *Appetite, 51*, 42–49.

Te Morenga, L. A., Mann, J., & Mallard, S. (2013). Dietary sugars and body weight: Systematic review and meta-analyses of randomised controlled trials and cohort studies. *British Medical Journal, 346*, e7492.

te Poele, E. M., Devlamynck, T., Jäger, M., Gerwig, G. J., Van de Walle, D., Dewettinck, K., ... Dijkhuizen, L. (2018). Glucansucrase (mutant) enzymes from *Lactobacillus reuteri* 180 efficiently transglucosylate *Stevia* component rebaudioside A, resulting in a superior taste. *Scientific Reports, 8*, 1516 1038/s41598-018-19622-5.

Tukey, J. W. (1953). *The problem of multiple comparisons.* Princeton University.

Van Leeuwen, S. S., Leeflang, B. R., Gerwig, G. J., & Kamerling, J. P. (2008). Development of a ^{1}H NMR structural-reporter-group concept for the primary structural characterization of α-D-glucans. *Carbohydrate Research, 343*, 1114–1119.

Wang, Y., Chen, L., Li, Y., Li, Y., Yan, M., Chen, K., ... Xu, L. (2015). Efficient enzymatic production of rebaudioside A from stevioside. *Bioscience, Biotechnology, and Biochemistry, 80*, 67–73.

World Health Organization. The challenge of obesity in the WHO European Region and the strategies for response. (2007). http://www.who.int.

Yu, X., Yang, J., Li, B., & Yuan, H. (2015). High efficiency transformation of stevioside into a single mono-glycosylated product using a cyclodextrin glucanotransferase from *Paenibacillus* sp. CGMCC 5316. *World Journal of Microbiology and Biotechnology, 31*, 1983–1991.